WELDING RESEARCH

Strain-Based Heating of Polymers under Ultrasonic Excitation

An investigation of the physical properties that affect viscoelastic heating of polymers under ultrasonic vibration

BY M. MARCUS AND E. SANCAKTAR

Abstract

Ultrasonic welding is the most common type of polymer joining used in industry today. It is critical that the energy transfer and heating mechanisms be well understood to enable the use of this process for more challenging applications. This work seeks to provide new tools to predict the heating rate in a molded polymer part excited by ultrasonic energy. Current assumptions for the mechanics of energy transfer are explored, and new equations for attenuation and strain-based heating are proposed.

Keywords

- Ultrasonic Plastic Welding
- Ultrasonic Attenuation
- Ultrasonic Heat Generation

Introduction

Ultrasonic heating of a polymer relates to the out-of-phase relationship of the stress and strain waves in the material, an effect of viscoelasticity. The losses generated by this out-of-phase behavior cause heating, and the loss magnitude depends on the material's ultrasonic frequency, amplitude, and loss modulus. These losses also lead to attenuation, a reduction in amplitude, so that the amplitude of vibration at the joint is less than that at the surface where the ultrasonic wave is initially applied to the part (Ref. 1).

The main components of an ultrasonic welding system are shown in Fig. 1. The ultrasonic vibrations that initiate heating are applied via an ultrasonic stack. This stack consists of three components: a transducer (a converter), a booster, and a horn (a sonotrode). The transducer converts a high-frequency electrical signal from a generator into mechanical motion via piezo-electric ceramics that expand and contract in response to electrical impulses. The booster is used to either increase or decrease the amplitude of the vibrations depending on its mass ratio. The horn is configured to apply vibrations to the top surface of the plastic part over the joint (Ref. 2).

The ultrasonic stack is used to compress two polymer components placed in physical contact such that the ultrasonic vibrations are traveling perpendicular to the faying surface. The generated polymer melt is pushed away from the joint as force is applied. This step exposes a new solid-to-solid contact surface to generate more heating from vibrations. This cyclical process continues until the weld feature completely melts (Ref. 2).

The amplitude at the sonotrode face can be calculated based on the amplitude of the transducer, a value typically provided by the equipment supplier, and the expected gain of the booster and sonotrode based on their geometry. Gain is simply the ratio of the mass of the ultrasonic tool, such as the booster or sonotrode, before the nodal point versus after. As the wave passes through the component, the magnitude of the lengthwise deformation can be increased by reducing the mass present on the part's second quarter wavelength.

Because the ultrasonic sonotrode has the same density throughout, the gain can be calculated as the ratio of the cross-sectional area where the ultrasonic wave enters the sonotrode to the cross-sectional area where the ultrasonic wave exits the sonotrode. Figure 2 shows how this can be calculated using the example of an ultrasonic sonotrode with a rectangular front and a cylindrical back. The 0.8 factor is an estimated adjustment to account for the transition radius between the front and back of the sonotrode.

Experimentally, this calculated amplitude can be confirmed via optical or mechanical measurements. A mechanical approach is shown in Fig. 3. A standard displacement gauge can be placed in contact with the bottom surface of the sonotrode and zeroed. At this point, the ultrasonics can be activated using the "test" function of the ultrasonic generator. The response rate of the gauge is not fast enough to follow the motion of the ultrasonic sonotrode face, so a maximum value is displayed at

https://doi.org/10.29391/2025.104.001

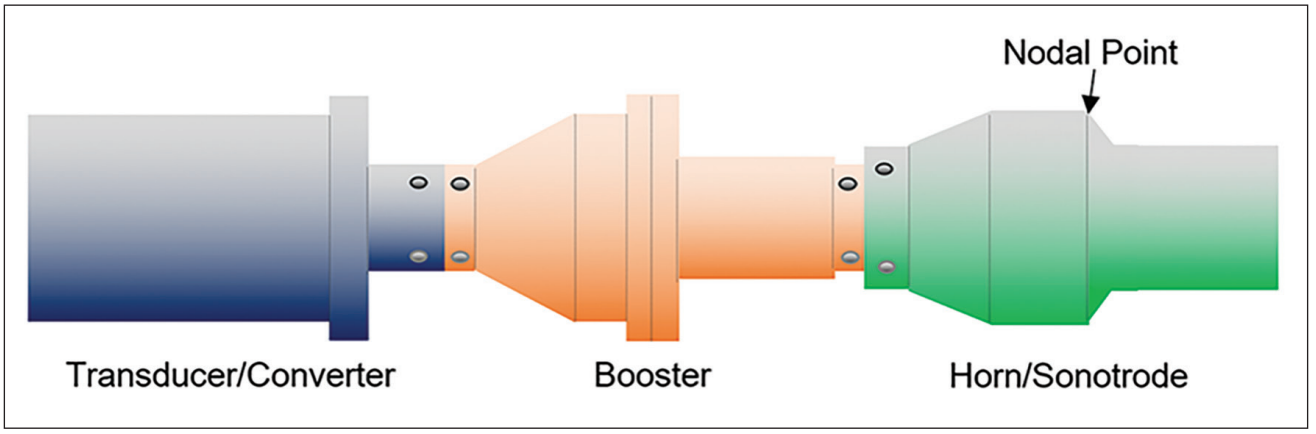

Fig. 1 — Ultrasonic stack diagram.

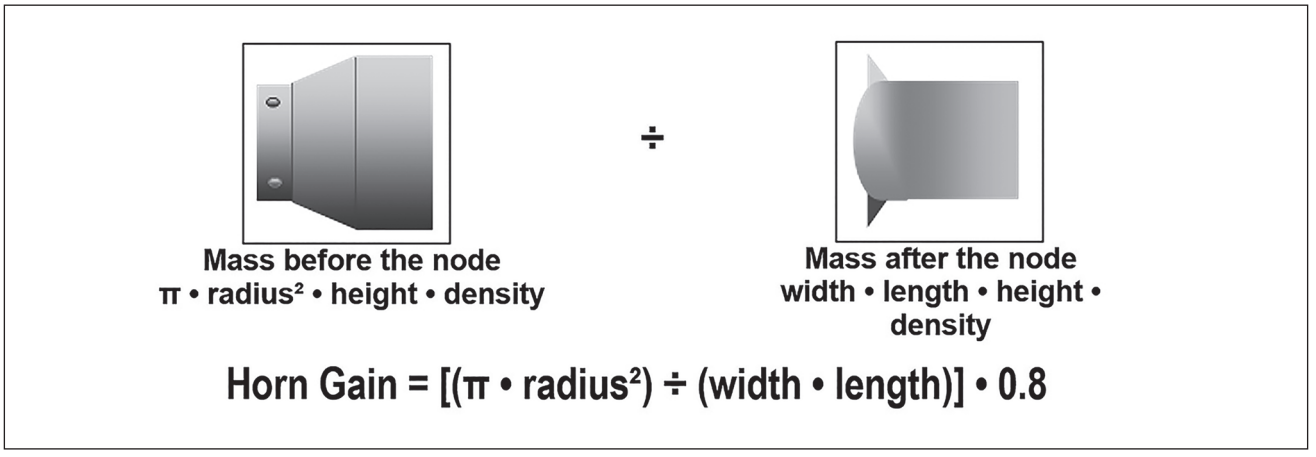

Fig. 2 — Method to calculate the gain of an ultrasonic component.

the maximum expansion of the sonotrode, which is equivalent to the 0-peak amplitude at the sonotrode face.

While the amplitude of vibration at the face of the ultrasonic sonotrode can be easily calculated and measured as described, it is more challenging to find the amplitude of the ultrasonic vibration at the weld joint interface.

If one assumes a simple bar or rod model, the ultrasonic wave transfers linearly through the polymer. The amplitude at the joint will then be affected by two phenomena: the wave's phase at the joint location and attenuation.

The wave phase at the joint location will depend on the velocity of the ultrasonic wave in the polymer and the distance from the sonotrode contact surface to the joint. The vibration wave will have a maximum amplitude at the sonotrode contact surface.

The amplitude of vibration at the weld joint has typically been used as the instantaneous deformation in the polymer to calculate heat generation. However, this approach neglects the effects of the part geometry and the force applied to the heating rate. In this work, the key components of ultrasonic heating are vibration amplitude, the mechanism of ultrasonic heating, and how strain is determined. Each of these is independently discussed, including the derivation of a simplified equation to predict the amplitude at the weld joint accounting for attenuation and phase shift. The strain heating mechanism for plastic welding is also evaluated and a new approach for estimating strain is proposed.

Background and Theory

Vibration Amplitude within Polymer

Attenuation is the loss of amplitude of the ultrasonic wave as it travels through a polymer due to the imperfect transfer of the vibrations through a viscoelastic material. While elastic materials (i.e., metals) are generally assumed to provide near perfect transfer of vibrations, the viscous portion of plastics does not transfer vibrations. The viscous portion of the polymer absorbs kinetic energy (resulting in heating), while the elastic portion transfers it, leading to an overall loss of peak amplitude (Ref. 3).

This viscoelastic response of polymers to mechanical deformation can be visualized as a spring and dashpot system. The most common models of this type are the Maxwell and Kelvin-Voight models. The idea is that polymers have both an elastic response, represented by a spring, and a viscous response, represented by a dashpot. Imagine pulling on the

Fig. 3 — Method for measuring amplitude at the ultrasonic sonotrode face using a displacement gauge.

end of the system depicted in Fig. 4; at high rates, the spring will present less resistance to movement than the dashpot. Similarly, some mechanical energy is transferred quickly and efficiently in plastics, but some is not (Refs. 4, 5). It is this resistance to transfer that causes a loss in ultrasonic amplitude at the weld joint due to attenuation — and it is also this loss that causes vibrations in polymers to generate heating.

Several methods of estimating the loss in amplitude as the wave travels through a polymer have been proposed. Sancaktar describes a method to determine the nodal point in the polymer or the points at which there is zero or maximum vibration (Ref. 6). This method is based on the description of ultrasonic waves as plane waves from the basic theory of elasticity. If a part has a simple geometry, the node points of the wave in the polymer can be predicted with the following equation:

$$L = \frac{V_L}{f} = \frac{1}{f}\left[\frac{E}{\rho}\frac{(1-v)}{(1+v)(1-2v)}\right]^{1/2} \quad (1)$$

where L is wavelength, V_L is the velocity of the wave propagation, f is frequency, E is Young's modulus, ρ is density, and v is Poisson's ratio.

If the distance from the sonotrode contact surface to the joint is L/2 (half wavelength), then very little or no amplitude will be available, resulting in a weak or no weld. If the part has a complex geometry, computer modeling is more efficient in determining the location of nodal points.

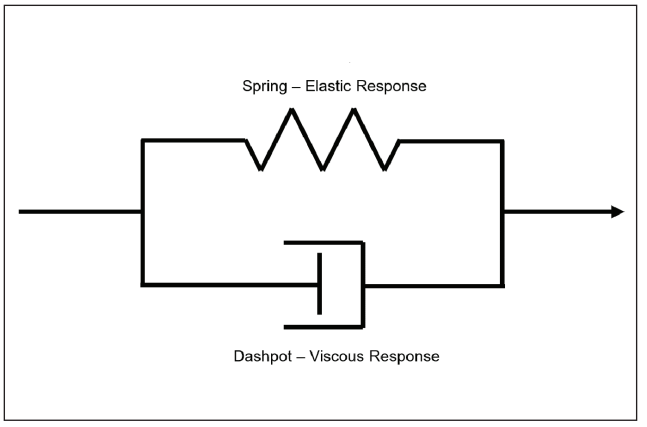

Fig. 4 — Kelvin-Voight model of viscoelastic response.

While this approach is very helpful to find the wavelength of the ultrasonic vibrations in a polymer, it cannot be used to find amplitude at a specific distance. Additionally, it only accounts for the phase of the wave and does not account for attenuation. However, it is useful during designing to determine optimum distances from the sonotrode contact surface to the weld joint or distances to be avoided.

Suresh et al. proposed that the attenuation of the ultrasonic wave in polymers, represented as a logarithmic decrease, can be applied to ultrasonic welding (Ref. 7). This model was originally proposed for use in ultrasonic nondestructive testing of plastics to model the response rate for low-power vibrations (Ref. 8). Following this method, the attenuation of the plastic material can be approximated by the equation:

$$2\alpha z = 20 \log \frac{I_0}{I} \quad (2)$$

where α is the attenuation coefficient, z is the distance traveled by the wave, I_0 is the initial amplitude, and I is the final amplitude (Ref. 7).

For most weldable thermoplastics at 20 kHz and room temperature, the attenuation coefficient is generally in the range of ten to 100 (Ref. 8). The drawback to this method of modeling attenuation is that a specific coefficient must be measured for each material of interest.

An alternative method of calculating the attenuation of ultrasonic energy as the wave travels through a plastic part is proposed by Sancaktar, based closely on the Kelvin-Voight model of viscoelastic response (Ref. 6).

From this model, the following equation of transmissibility of the vibrations can be developed:

$$T_r = \frac{F_t}{F_0} = \frac{[E^2 + (\eta\omega_f)^2]^{1/2}}{[(E - m\omega_f^2)^2 + (\eta\omega_f)^2]^{1/2}} \quad (3)$$

where T_r is transmissibility, F_t is transmitted force, F_0 is exciting force, E is the elastic modulus, η is viscosity, ω_f is the forcing frequency, and m is the mass of the system (Ref. 6).

For a constant cross section, T_r is also equal to the ratio of the transmitted stress to the exciting stress. And, because Stress (σ) = Modulus (E) * Strain (ε), T_r is also equal to the ratio of transmitted strain (amplitude at the joint) to exciting strain (amplitude delivered by the ultrasonic sonotrode) within the same material.

This second method relieves the need to define an attenuation coefficient experimentally and relates to properties that can be easily measured.

Alternatively, Benatar and Cheng proposed and validated an approach to account for both phase shift and attenuation effects in a single equation based on the 1D-bar wave equation (Refs. 9, 10):

$$u(x,t) = u_0 e^{-\alpha x} e^{-i\omega\left(\frac{x}{v}-t\right)} \quad (4)$$

where u(x,t) is the amplitude of the wave as a function of time (s), t, and distance (mm), x, from the sonotrode contact surface; u_0 is the amplitude (mm) at x = 0 (at the sonotrode contact surface); ω is the frequency (cycles/s), and α is the unitless attenuation factor:

$$\alpha = \frac{\omega\sqrt{\rho E^{IV}}}{|E^*|} \quad (5)$$

and v is the phase velocity (1/s):

$$v = \frac{|E^*|}{\sqrt{\rho E^{III}}} \quad (6)$$

where ρ is the density, E* is the complex modulus, and E^{III} and E^{IV} are related to loss and storage modulus:

$$E^{III} - iE^{IV} = \sqrt{E' - iE''} \quad (7)$$

However, rearranging the presentation can simplify the equation as described below. The first step is to eliminate the imaginary component and to present a single equation in terms of commonly measured material properties. Note that the relationship of E^{III} and E^{IV} to the loss and storage moduli can also be expressed by the following two equations:

$$E^{III} = \sqrt{|E^*|}\cos\left(\frac{\delta}{2}\right) \quad (8)$$

$$E^{IV} = \sqrt{|E^*|}\sin\left(\frac{\delta}{2}\right) \quad (9)$$

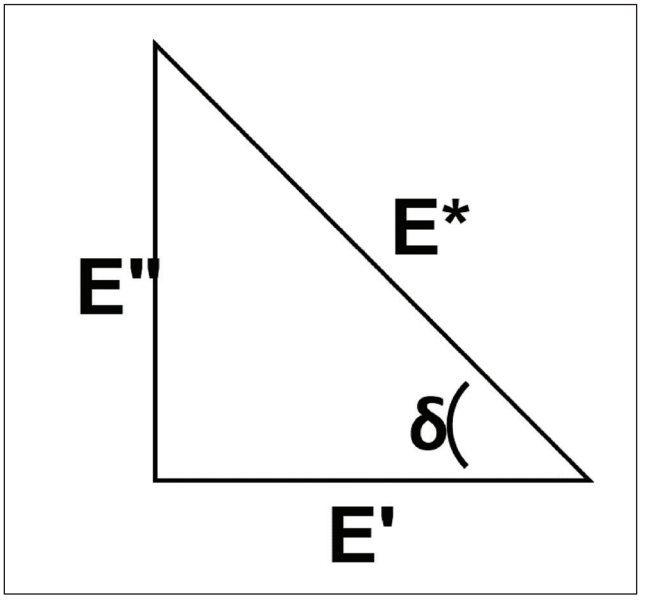

Fig. 5 — Geometric relationship between loss and storage: E" — the loss modulus; E' — the storage modulus; E — the complex modulus; δ — the loss factor.*

where δ is the damping factor (tanδ = E"/E'), and E* is the complex modulus:

$$|E^*| = \sqrt{E'^2 + E''^2} \quad (10)$$

A simplification of Equation 4 is proposed via the following process. To predict heat generation, only the maximum peak-to-peak amplitude is needed, so the equation can be isolated at a single point in time, when the ultrasonic wave is at the maximum amplitude, at t = 0. Therefore, Equation 4 can be simplified to the following:

$$u(x) = u_0 e^{-\alpha x} e^{-i\omega\left(\frac{x}{v}\right)} \quad (11)$$

By applying Euler's relation (Equation 12) to the phase shift portion of Equation 11, it can be further simplified as shown in Equations 13–14:

$$e^{ix} = \cos x + i\sin x \quad (12)$$

$$e^{-i\omega\left(\frac{x}{v}\right)} = \cos\left(\frac{-\omega}{v}x\right) + i\sin\left(\frac{-\omega}{v}x\right) \quad (13)$$

$$Real\left[\cos\left(\frac{-\omega}{v}x\right) + i\sin\left(\frac{-\omega}{v}x\right)\right] = \cos\left(\frac{-\omega}{v}x\right) \quad (14)$$

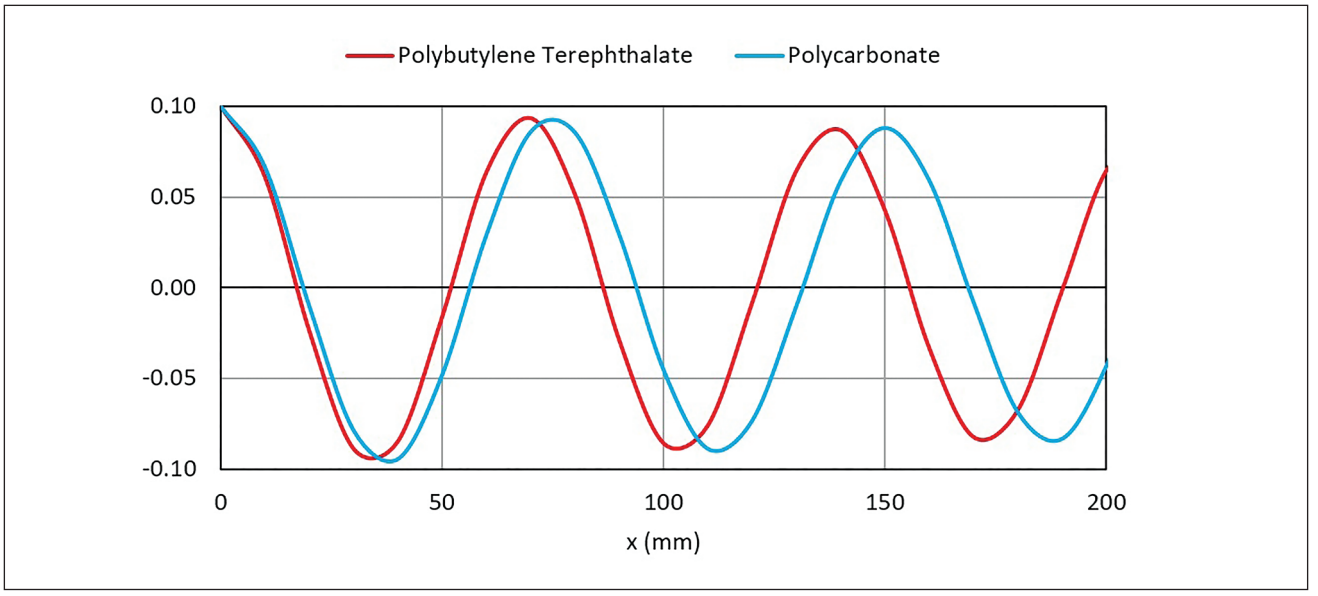

Fig. 6 — Peak-to-peak amplitude (mm) vs. distance from sonotrode contact surface, x (mm), for two polymers.

Thus, Equation 11 can be written as:

$$u(x) = u_0 e^{-\alpha x} \cos\left(\frac{-\omega}{v} x\right) \tag{15}$$

While this equation eliminates the imaginary component and allows for calculation of maximum amplitude vs. distances, instead of amplitude vs. time at each distance, it is also desired to eliminate the unwieldy E^{III} and E^{IV} material properties from the equation. These material properties are not well known or commonly used.

To begin the elimination process, the long form of the attenuation coefficient and the phase shift factor are applied to Equation 15:

$$u(x) = u_0 e^{-\frac{\omega\sqrt{\rho}E^{IV}}{|E^*|}x} \cos\left(\frac{-\omega}{\frac{|E^*|}{\sqrt{\rho}E^{III}}} x\right) \tag{16}$$

Next, the long forms of the E^{III} and E^{IV} material properties are inserted into the equation:

$$u(x) = u_0 e^{-\frac{\omega\sqrt{\rho}\sqrt{|E^*|}\sin\left(\frac{\delta}{2}\right)}{|E^*|}x} \cos\left(\frac{-\omega}{\frac{|E^*|}{\sqrt{\rho}\sqrt{|E^*|}\cos\left(\frac{\delta}{2}\right)}} x\right) \tag{17}$$

The complex modulus in the fractions can be simplified by manipulating the exponent by:

$$\frac{|E^*|}{\sqrt{|E^*|}} = \frac{|E^*|}{|E^*|^{0.5}} = |E^*|^{1-0.5} = |E^*|^{0.5} = \sqrt{|E^*|} \tag{18}$$

And the fraction in the cosine can be simplified so that Equation 17 becomes:

$$u(x) = u_0 e^{-\frac{\omega\sqrt{\rho}\sin\left(\frac{\delta}{2}\right)}{\sqrt{|E^*|}}x} \cos\left(\frac{-\omega\sqrt{\rho}\cos\left(\frac{\delta}{2}\right)}{\sqrt{|E^*|}} x\right) \tag{19}$$

By changing the variable "u" to "A" to align with the variable definitions in this work and by assigning two new variables to the equation components to simplify writing it, Equation 19 can now be written as:

$$A(x) = A_0 \cos(Dx \cos\phi)\, e^{(Dx \sin\phi)} \tag{20}$$

where A(x) is the function of maximum peak-to-peak amplitude as a function of distance into the material, A_0 is the peak-to-peak amplitude at the sonotrode contact surface, and ϕ is the unitless phase shift factor:

$$\phi = \frac{\delta}{2} = \frac{1}{2}\tan^{-1}\frac{E''}{E'} \quad (21)$$

and D is the damping coefficient:

$$D = \frac{-\omega\sqrt{\rho}}{\sqrt{|E^*|}} \quad (22)$$

A dimensional analysis of the damping coefficient, D, shows that this factor is also unitless:

$$D = \frac{\frac{1}{s} * \sqrt{\frac{g}{cm^3}}}{\sqrt{\frac{g}{s^2 * cm^3}}} \quad (23)$$

Thus, we have an equation for amplitude in terms of initial amplitude (amplitude at the sonotrode contact surface) multiplied by a ratio that varies with distance per the phase of the wave as well as per the loss in vibration energy due to viscous damping.

However, while Equation 20 eliminates the unwieldy E^{III} and E^{IV}, it is unclear how the damping and phase shift relate to the relevant material properties. Thus, further modification of the equation was pursued. First, consider the standard equation for wavelength:

$$\lambda = \frac{c}{f} \quad (24)$$

where c is the speed of sound in the medium and f is the frequency of the wave.

The speed of sound is given by the equation:

$$c = \sqrt{\frac{K}{\rho}} \quad (25)$$

where K is the material property relating to the sound propagation in the medium and ρ is the density.

In the case of ultrasonic wave propagation through a polymer, the relevant material property is the complex modulus. Referring to Equation 23, the damping coefficient, D, is a function of the wavelength and can be rewritten as:

$$D = \frac{-\omega\sqrt{\rho}}{\sqrt{|E^*|}} = \frac{-\omega}{c} = \frac{-1}{2\pi\lambda} \quad (26)$$

Next, consider cosΦ and sinΦ from Equation 20 and the definition of Φ from Equation 21. Figure 5 shows the geometry described by these geometric equations.

This illustrates the fundamental relationship described in Equations 27 and 28 below:

$$\tan\delta = \frac{E''}{E'} \quad (27)$$

$$|E^*| = \sqrt{E'^2 + E''^2} \quad (28)$$

Thus, sinΦ can be rewritten as:

$$\sin\phi = \sin\frac{\delta}{2} = \frac{1}{2}\frac{E''}{E^*} \quad (29)$$

And cosΦ is:

$$\cos\phi = \cos\frac{\delta}{2} = \frac{E'}{E^*} \quad (30)$$

Thus, the equation for amplitude as a function of distance becomes Equation 31:

$$A(x) = A_0 \cos\left(\frac{-2\pi x E'}{\lambda E^*}\right) e^{\frac{-\pi x E''}{\lambda E^*}} \quad (31)$$

This arrangement is preferred as each component is a commonly used and established parameter that does not require the definition of additional variables.

Further, when written in this format, the relationship between each component of the equation and its operator becomes clearer. The exponential decay of the ultrasonic wave amplitude is guided by the loss modulus of the material and the wavelength, which is appropriate and reasonable. The cosine component establishes the phase of the wave as it passes through the material, and this phase shifts in relation to the storage modulus and wavelength.

Ideally, the loss modulus (E') and storage modulus (E") of the material would be measured at, or extrapolated for, the frequency of vibration being used in the ultrasonic welding process. When using values that have been established previously for two polymers (Ref. 11), the graph shown in Fig. 6 can be produced.

Equation 31 can be simplified even further as the factor of E'/E* in the cosine function is nearly one for most polymer welding applications. Therefore, it can be eliminated, resulting in Equation 32:

$$A(x) = A_0 \cos\left(\frac{-2\pi x}{\lambda}\right) e^{\frac{-\pi x E''}{\lambda E^*}} \quad (32)$$

where A(x) is the function of maximum peak-to-peak amplitude as a function of distance into the material, A_0 is the peak-to-peak amplitude at the sonotrode contact surface, λ is the wavelength in the polymer, E" is the loss modulus, and E* is the complex modulus.

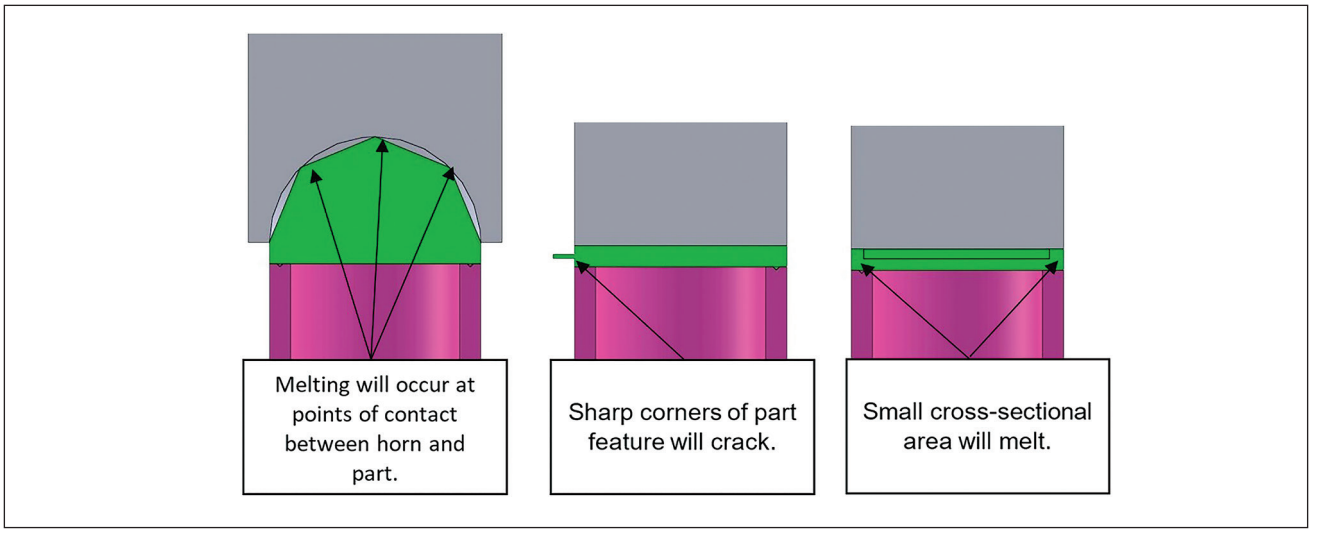

Fig. 7 — Diagram showing how the ultrasonic vibration affects areas outside the joint.

Heating Due to Ultrasonic Energy within Polymer

This amplitude calculation can be incorporated into the heat generation equation for ultrasonic welding. A derivation of this heating equation is described below for two reasons. First, to provide the first principles context for this paper, and second, to verify the units of the equation. With regard to the unit verification, this equation is often reported without the note that Q is the energy generated per volume, which is clarified here.

During the ultrasonic vibration of a polymer, the energy input into the joint of the plastic part is due to the mechanical deformations caused by the ultrasonic vibrations. To define this heating, we can start with the fundamental definition of work, W:

$$W = Fd \tag{33}$$

where F is the force applied, and d is the displacement over which the force is applied.

In ultrasonic welding, the force being applied is cyclical and is applied over very small deformations. Since the deformations are so small, we can assume linear viscoelastic properties govern the interaction. For the case of linear viscoelasticity, there is a direct relationship between stress and strain in the material when expressed in the Laplace Transform domain, i.e.,

$$\sigma(s) = E^*(s)\varepsilon(s) \tag{34}$$

where $\sigma(s)$ is the stress, $E^*(s)$ is the modulus, and $\varepsilon(s)$ is the strain expressed in Laplace Transform Domain.

The modulus, $E^*(s)$ of Equation 34, which describes how much of the vibrations are transferred, is called the complex modulus and is made up of a storage and a loss modulus. The storage modulus describes how much of the vibrational energy is transferred, and the loss modulus describes how much energy is dissipated as heat.

These moduli are typically measured using dynamic mechanical analysis. It is important to note that the storage and loss moduli are functions of both temperature and frequency of vibration. A constant modulus analytical approach simplifies modeling the heating behavior of polymers under ultrasonic vibration. The constant storage and loss moduli approach uses the moduli at room temperature and the driving frequency of the system. Previous research has shown this to be a valid approach (Refs. 11, 12).

It is, however, important to note that this approximation is being made, typically using material properties measured at lower frequencies via dynamic mechanical analysis (DMA) and extrapolated to higher frequencies through time temperature superposition (TTS). This approximation is known to be imperfect, but it has been the only available approach historically. However, recent research has suggested a much more accurate approach using custom high-frequency activation accompanied by simulation to extract the material properties based on observed effects (Ref. 13).

Now, from the definition of stress, we know that:

$$\sigma = F/a \tag{35}$$

where σ is the stress, F is the force being applied, and a is the area over which it acts.

From the definition of strain, it is known that:

$$\varepsilon = \frac{\delta x}{dx} \tag{36}$$

where ε is the strain, δx is the displacement, and dx is the reference length of the object being acted on. In our case,

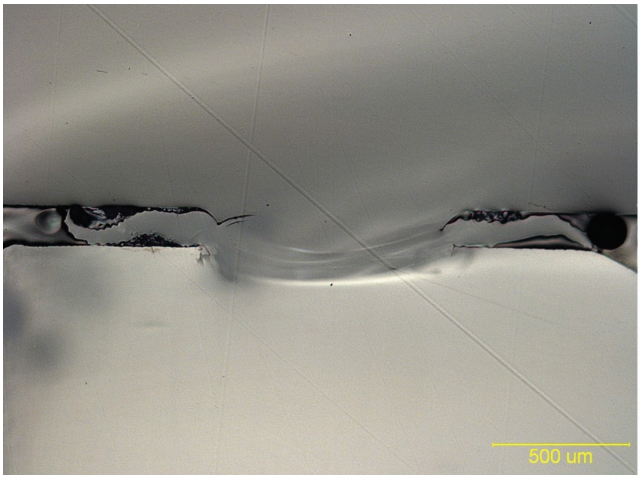

Fig. 8 — Cross section of weld joint with partially melted energy director.

we take the reference length as the energy director height on the plastic part.

Equations 34–36 can be combined:

$$W = \sigma a * \varepsilon dx \tag{37}$$

$$\frac{W}{adx} = \sigma * \varepsilon \tag{38}$$

where W is work, a is the area, dx is the instantaneous reference length, σ is the stress, and ε is the strain.

To find the work per volume per vibration cycle, the stress and strain are integrated over a single cycle, 0 to 2π/ω:

$$\frac{W}{V} = \int_0^{\frac{2\pi}{\omega}} \sigma \, d\varepsilon \, dt \tag{39}$$

During ultrasonic vibration, deformation is applied cyclically, which can be modeled as following a cosine wave:

$$\varepsilon(t) = \varepsilon_0 cos\omega t \tag{40}$$

where ε_0 is the 0-peak maximum amplitude at the beginning of the cycle.

Thus, the storage modulus, or transferred portion of the ultrasonic vibrations, can be assumed to follow this cosine. Conversely, the loss modulus, or out-of-phase portion of the ultrasonic vibrations, can be assumed to follow the sine:

$$E^* = E'cos\omega t - E"sin\omega t \tag{41}$$

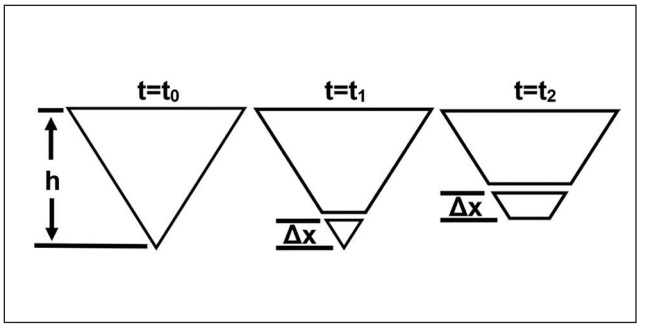

Fig. 9 — Diagram of how melt progresses over time in the energy director.

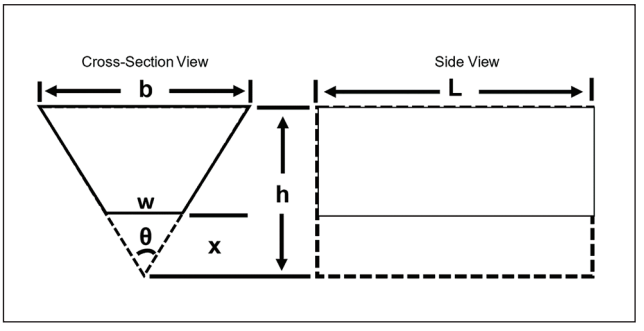

Fig. 10 — Diagram of energy director geometry after some melting has occurred.

Physically, this means that at t = 0, the strain is equivalent to the maximum deformation induced by the ultrasonic vibration, ε_0. After this, the strain diminishes and grows with the vibration cycle.

Subsequently, the stress is given by:

$$\sigma = E^*\varepsilon = (E'cos\omega t - E"sin\omega t)\varepsilon_0 \tag{42}$$

Physically, this means that at t = 0, the stress is equal to the storage modulus times the initial (maximum) strain, and thereafter, it varies according to the complex modulus.

Combining Equations 39 and 42, the equation becomes:

$$\frac{W}{V} = \int_0^{\frac{2\pi}{\omega}} [E'cos\omega t - E"sin\omega t)\varepsilon_0][-\varepsilon_0 \omega sin\omega t] \, dt \tag{43}$$

Following the steps of integration, this equation simplifies to:

$$\frac{W}{V} = \pi E"\varepsilon^2 \tag{44}$$

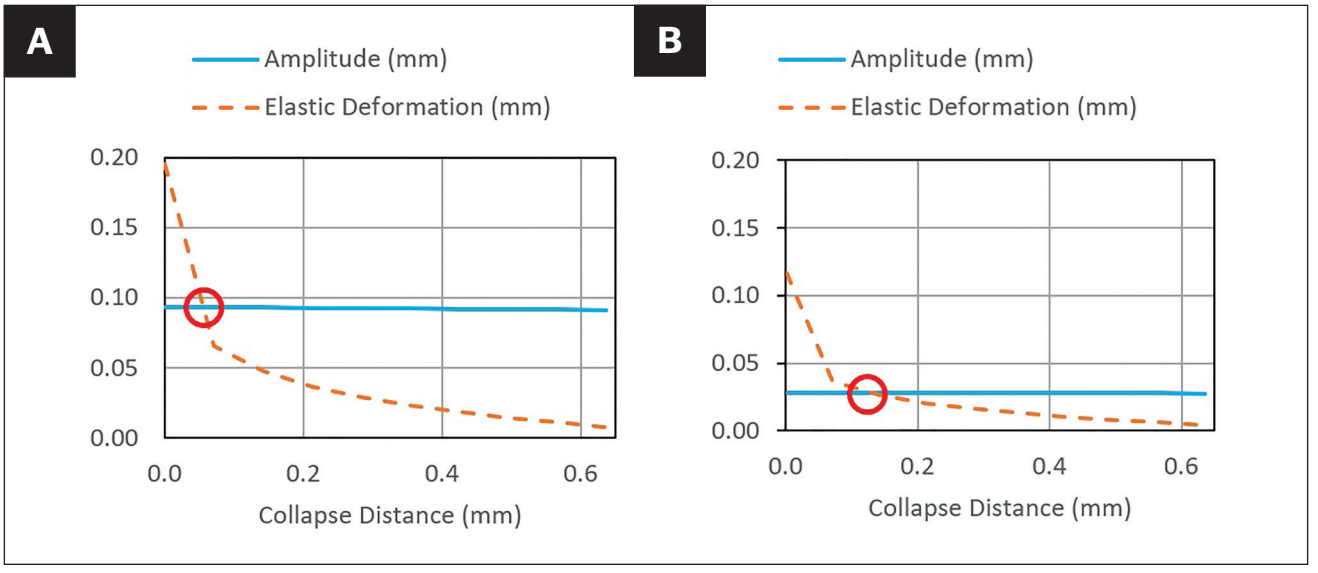

Fig. 11 — Amplitude and elastic deformation (mm) vs. collapse distance (mm) for a part with a 60-deg energy director: A — Polybutylene terephthalate (PBT), 0.1-mm amplitude input; B — polycarbonate (PC), 0.03-mm amplitude input.

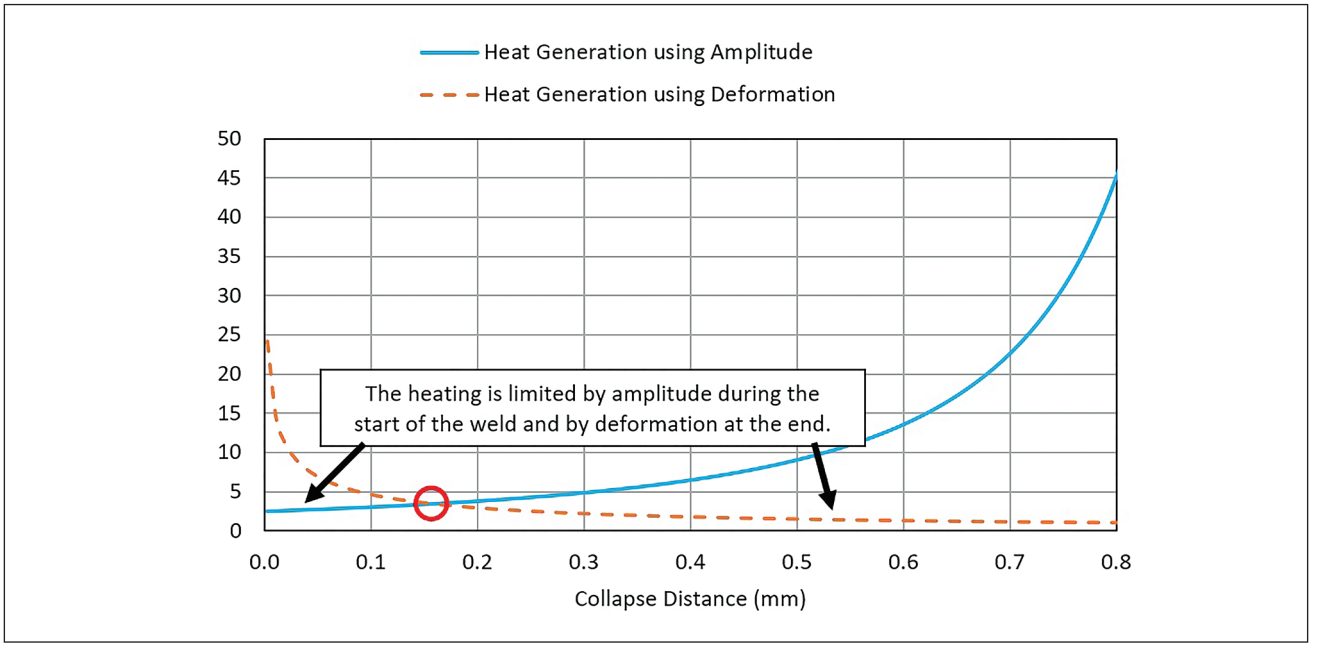

Fig. 12 — Internal heat generation rate (J/cm³/s) calculated using the amplitude at the joint vs. calculated using pressure-induced deformation as a function of collapse distance for a 1-mm-wide polycarbonate (PC) energy director.

This gives the work per volume per cycle. To find the average work, or average energy dissipation (Q) per volume into the plastic, the equation is multiplied by the period (ω/2π):

$$\frac{Q}{V} = \frac{1}{2}\omega E'' \varepsilon^2 \tag{45}$$

where Q is the heat generation rate, V is the volume, ω is the frequency in radians, E" is the loss modulus, and ε is the strain.

A dimensional analysis of Equation 45 is given below, for reference:

$$\frac{Joules/sec}{cm^3} = \frac{1}{2}\left(\frac{1}{sec}\right)\left(\frac{Joules}{cm^3}\right)\left(\frac{cm}{cm}\right) \tag{45A}$$

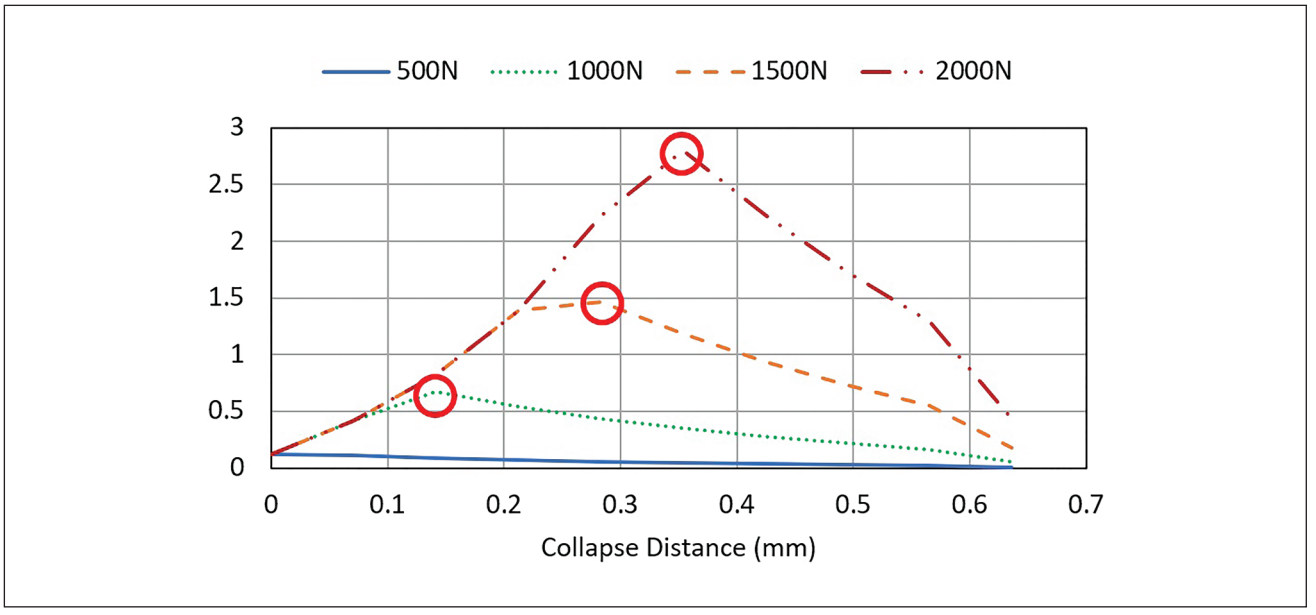

Fig. 13 — Heat generation rate (J/s) vs. collapse distance (mm) when elastic deformation limit is included for polycarbonate (PC) at various loads.

It is convenient to employ units of cm in this equation due to the small size of the volume being heated. Additionally, the loss modulus is typically found in terms of MPa, which is equivalent to J/cm^3.

Strain for the Heat Generation Equation

An engineering strain is typically used in the heat generation equation (Equation 45). This engineering strain is approximated as the amplitude produced at the joint divided by the energy director height. However, this approximation does not account for the effect of force and geometry on heat generation.

Experimentally, it has been shown that the energy director tip heats faster than nearby geometry. This is to be expected as the apex of the triangular energy director is subject to high-stress concentration when contacting the joint surface under force. Chuah et al. applied thermocouples to various points in a part and showed that the heating in the assembly is significantly concentrated at the energy director (Ref. 14).

However, using the energy director height as the reference length for the strain does not explain the heat generation when using no energy director. It is known that heating occurs throughout the part in contact with the ultrasonic sonotrode because heating of the entire part under ultrasonic activation is seen. For example, areas of a small cross section outside the joint can fracture, the sonotrode contact surface may melt, and sharp corners crack. In several cases of ultrasonic welding applications, it has been noted that if the sonotrode contact surface has a sufficiently small cross-sectional area, it will heat even before the energy director heats. Figure 7 shows examples of where undesired heating can occur during ultrasonic welding.

These observations suggest that the portion of the system that undergoes the most elastic deformation is the area of greatest heat generation. Therefore, a new method of considering heat generation in the ultrasonic part is proposed. It uses the portion of the ultrasonically activated plastic part that undergoes large elastic deformation under the applied force.

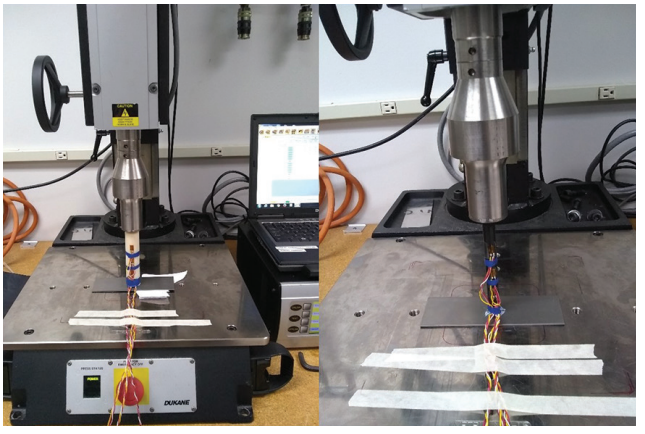

Fig. 14 — Experimental setup for strain measurement on acrylonitrile butadiene styrene (ABS) rods with a 2.54 cm diameter (left) and a 1.27 cm diameter (right).

Generally, it is assumed that the entire energy director heats simultaneously and melts uniformly. This approximation is useful to help predict weld time, where the heat generation rate can be considered an average if the full energy director is welded. The approximation, however, is not representative of reality. With any incomplete weld cross section, unmelted geometry is visible at the base of the energy director. This is a clear indication that melt starts at the triangular tip of the energy director and only moves into the base of the energy director as the melt is pushed out into the joint. Figure 8

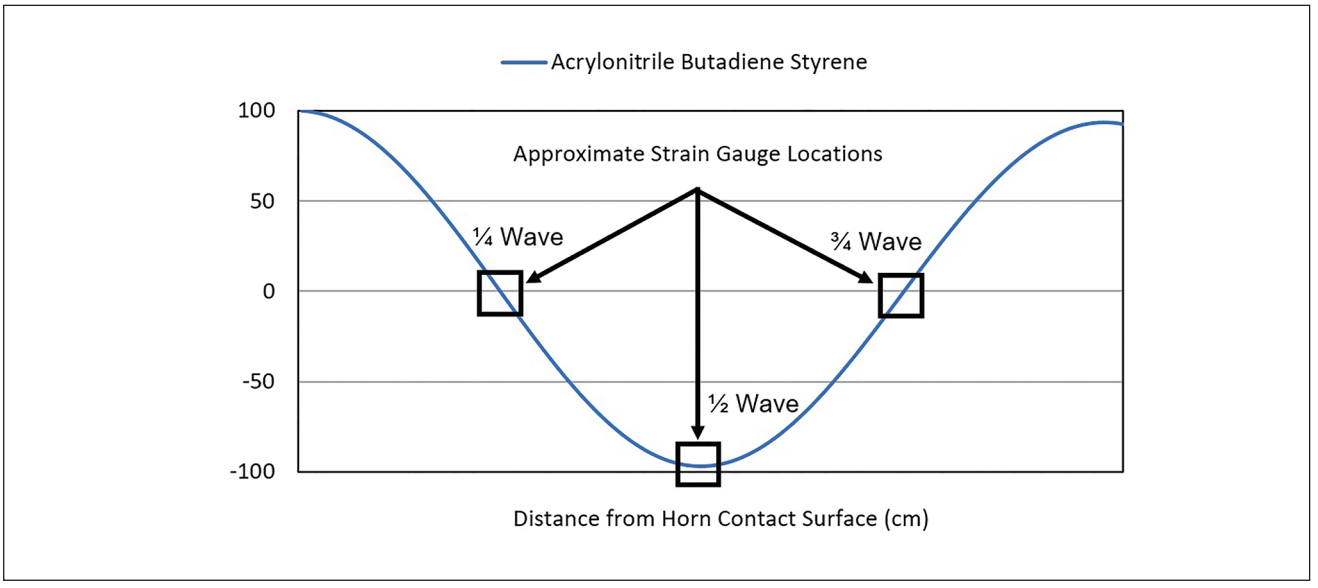

Fig. 15 — Placement of the strain gauges in relation to the expected percent of total amplitude of the ultrasonic wave at each location.

shows an example. Figure 9 shows how the energy director is expected to melt over time in discrete segments.

We note that the strain used in Equation 45 is not solely the amplitude over a function of energy director height. The maximum deformation can be approximated as the elastic deformation of the energy director, considering that any plastic deformation under the applied load will occur before ultrasonic energy is applied to the part.

This proposed approach to finding the deformation of the energy director under a static load begins with the stress-strain relationship:

$$\sigma = E\varepsilon \tag{46}$$

where σ is the stress, E is the modulus of elasticity, and ε is the strain:

$$\varepsilon = \frac{\delta x}{dx} \tag{47}$$

The stress is equal to the applied load (F) divided by the area (a), given by:

$$a = \frac{b}{h}xL \tag{48}$$

where b is the width of the energy director base, h is the height of the energy director, and L is the overall length of the energy director, as shown in Fig. 10.

Rearranging and integrating over the cross section:

$$\delta x = \frac{F}{E}\int_0^{x/h} \frac{1}{\frac{b}{h}xL} \tag{49}$$

which resolves to Equation 50:

$$\delta x = \frac{F}{E}\frac{h}{bL}\ln\left(\frac{x}{h}\right) \tag{50}$$

where F is the force applied, h is the energy director height, E is the elastic modulus, b is the energy director width, and L is the energy director length.

If we assume that insufficient force is applied to cause plastic deformation without ultrasonic vibration, then it makes sense that the actual effective amplitude is simply the elastic deformation of the energy director. However, the initial deformation of the energy director is limited by the amplitude of the ultrasonic wave at the joint.

Once the load is applied, the part has already experienced the deformation caused by the static load alone. Any further deformation is caused by the ultrasonic wave passing through the part. Therefore, while the sharp energy director geometry may allow significant elastic deformation, it cannot deform any more than the wave's amplitude at that location. This is especially important at the start of welding when the contact cross-sectional area of the energy director is still very small because the potential elastic deformation may be greater than the amplitude at that point.

Figure 11 compares the amplitude calculated using Equation 32 to find the amplitude at the weld joint vs. elastic deformation calculated per Equation 50 for two hypothetical scenarios. These are a 60-deg energy director on a (a) polybutylene terephthalate (PBT) part and (b) polycarbonate (PC) part. For this geometry and material, with an applied

Table 1 — Strain Gauge Specifications

Thermal Output Coefficients for 2024-T4 Aluminum at Gauge Factor of 2.00		Other
Order	Celsius	
0	−2.83E+1	Grid Resistance in Ohms: 120.0 +/− 0.3%
1	+2.56E+0	Gauge Factor at 24°C: 2.115 +/− 0.5%
2	−6.54E−2	Transverse Sensitivity: (+0.8 +/− 0.2)%
3	+3.56E−4	Temperature Compensation of Gauge Factor (%/100°C): (+1.3 +/− 0.2)
4	−3.85E−7	

Table 2 — Test Conditions

Rod Diameter (cm)	Force (N)	Ultrasonic Amplitude (microns)	Strain Gauge Locations Where Data Was Recorded
2.54	2224	0	¼, ½, ¾
		16	
		39	
	890	0	¼, ½
		16	
1.27	2224	0	¼, ½, ¾
		16	
		39	

load of 250 N assumed, the elastic deformation starts limiting the effective amplitude after about 10%-20% of the energy director is melted. This is at the crossover point where the amplitude at the joint and the deformation are equivalent, which is circled in Fig. 11.

When the deformation is used in the heat generation equation, the expected relationship of decreasing heat generation as the energy director collapses is predicted due to the increasing cross section of the energy director and reduction in the stress concentration on it. Conversely, when the traditional amplitude is used to calculate the strain in the heat generation equation, the predicted heating increases as the energy director collapses.

Figure 12 compares the two heat generation approaches (Equations 32 and 50 input into Equation 45) for PC. In this case, a 60-deg energy director on a PC part with an applied amplitude at the sonotrode face of 0.03 mm and a constant load of 250 N are assumed.

The smaller potential strain at each point in the weld process limits heat generation in the part. At the beginning of the weld, the amplitude is much less than the potential pressure-induced deformation. Thus, the heating is limited by the amplitude of the ultrasonic wave early in the weld cycle. As the energy director collapses, the joint's surface area increases, reducing the pressure-induced deformation to less than the amplitude of the ultrasonic wave. Thus, the heating is limited by the pressure-induced strain later in the weld cycle. The shift occurs at the cross-over point, as circled on Figs. 11 and 12.

When the strain is based on the applied weld pressure and joint geometry rather than amplitude, the rate of internal heat generation tapers down to zero as the energy director collapses fully. This is expected if the joint outside the energy director is large enough to have minimal elastic deformation under the applied load. However, it has been demonstrated experimentally that increasing amplitude does increase heating. This suggests that it may be appropriate to consider initial

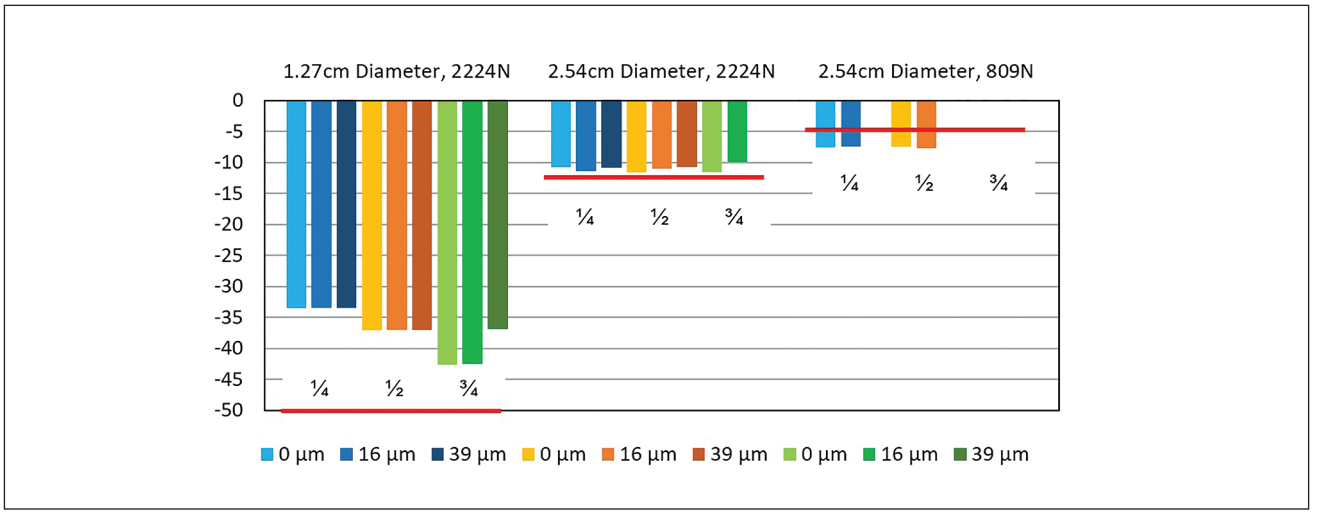

Fig. 16 — Measured displacement at three locations (¼, ½, ¾ wavelengths) using three amplitudes (0, 16, 39 µm) compared to the calculated elastic deformation (red lines).

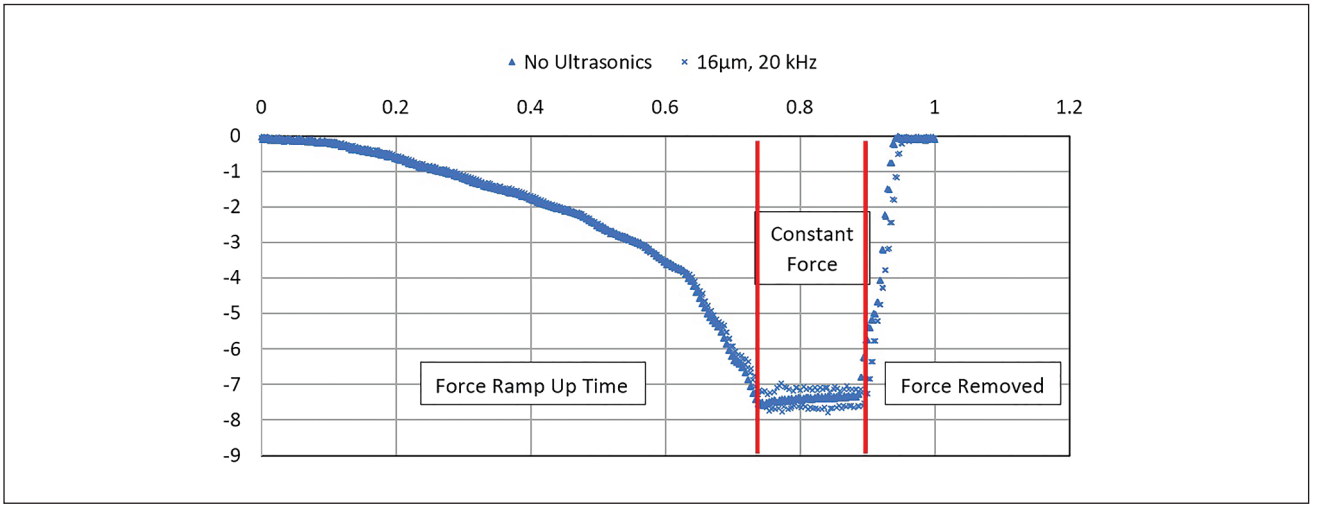

Fig. 17 — Displacement (µm) vs. time (s) for 2.54-cm-diameter rod at 890 N in the ¼ wave location.

heating to be controlled by the amplitude and later heating to be controlled by pressure-induced deformation. Due to the necessity of heating material from room temperature, initiating melt requires much greater energy input than maintaining melting since nearby material is already heated due to thermal conduction. This would explain the significant difference in weld time when amplitude is adjusted.

By accounting for the reduction in heating that occurs when elastic deformation is reduced, the noted effects of increased pressure and reduced contact area (by using an energy director at the joint instead of a flat contact surface) can be incorporated into the model. Figure 13 shows how pressure affects heating when accounting for elastic deformation. In this figure, the heating is calculated by limiting the achievable deformation at the joint to what is mechanically possible once this deformation is smaller than the amplitude of the ultrasonic wave at the joint. This crossover point is circled on Fig. 13 for each load.

The graph in Fig. 13 clearly shows that the initial heat generation increases monotonically at every force level but then drops off as the pressure-induced deformation starts limiting the effective strain at the energy director. The induced deformation is greater than the amplitude at higher pressure, even as the contact area widens as the energy director collapses. For this reason, the amplitude is less than the potential deformation for a longer period, and thus, the amplitude at the joint limits the effective strain at the energy director for more of the collapse distance. Because the pressure-induced deformation is greater at higher applied loads, the total energy input is greater when pressure is increased.

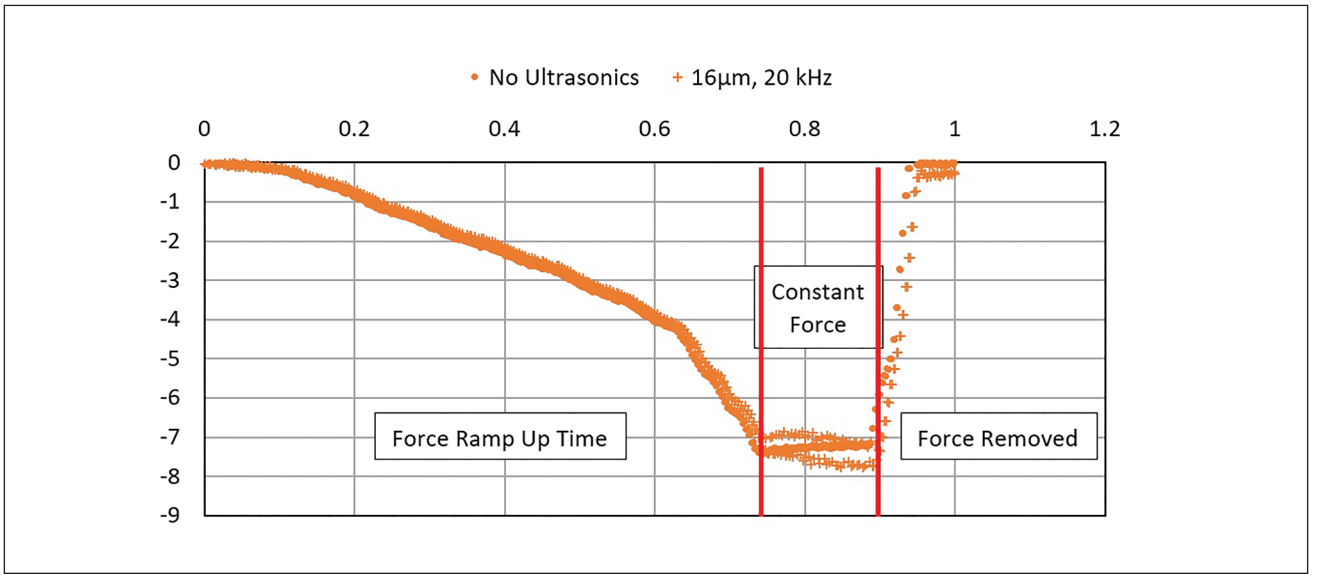

Fig. 18 — Displacement (µm) vs. time (s) for 2.54-cm-diameter rod at 890 N in the ½ wave location.

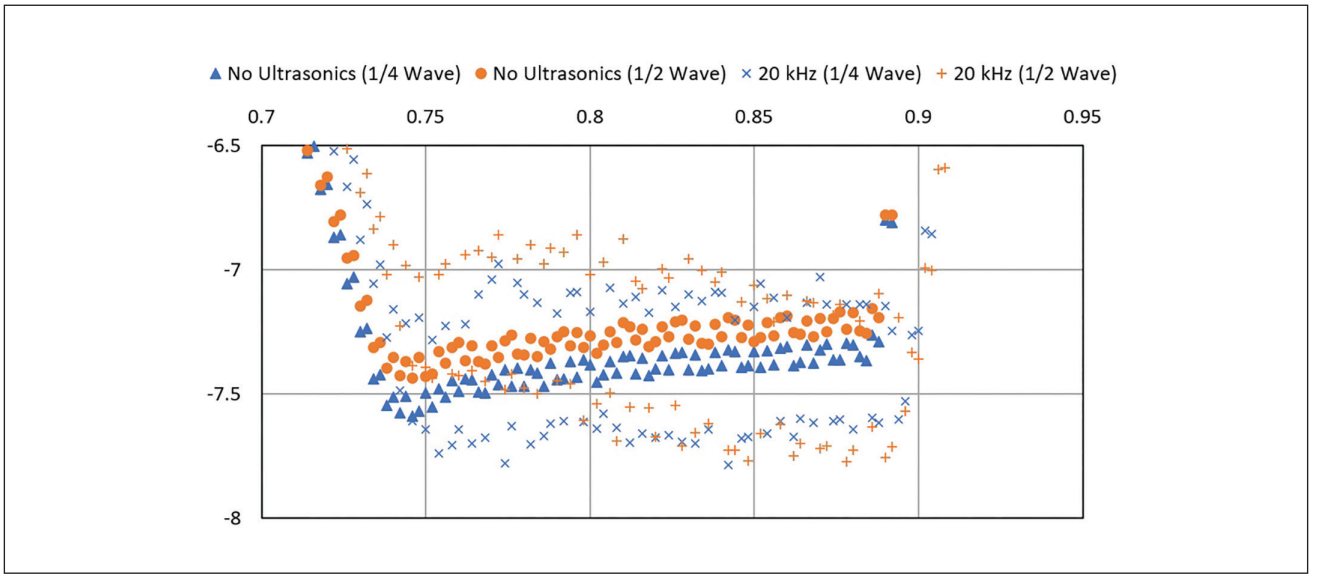

Fig. 19 — Displacement (µm) vs. time (s) for 2.54-cm-diameter rod at 890 N in the ¼ and ½ wave locations.

Experimentation

Methodology

It has been proposed that the actual change in length experienced by the plastic part is not limited by the amplitude but by the elastic strain that the part can experience under the applied load. To test this, strain gauges were used to measure the displacement in a polymer rod when compressed with and without ultrasonics. If the ultrasonic amplitude is transmitted through the rod independently of the applied load and geometry, then the measured displacement would correlate to the applied amplitude.

Two diameters of acrylonitrile butadiene styrene (ABS) rods were used: 1.27 cm and 2.54 cm. The rods were cut to about one full wavelength as calculated using Equation 51:

$$\lambda = \frac{c}{f} \tag{51}$$

where c is the speed of sound in the medium and f is the frequency of the wave.

The speed of sound for an ultrasonic wave passing through a polymer is given by the equation:

$$c = \sqrt{\frac{|E^*|}{\rho}} \tag{52}$$

For ABS, the modulus is 2.27 GPa (22,700,000,000 dyne/cc) and its density is 1.03 g/cc. Therefore, at 20 kHz, the wavelength in ABS is:

$$\lambda = \frac{\sqrt{\frac{|E^*|}{\rho}}}{f} = \frac{\sqrt{\frac{22700000000}{1.03}}}{20000} = 7.4\text{cm} \quad (53)$$

High-accuracy CEA-13-250UW-120 strain gauges from micro measurements with the specifications listed in Table 1 were used for testing. These strain gauges have a length of 0.635 cm and are accurate to about 5% for frequencies up to 40 kHz (Ref. 15).

As the wave travels through the polymer rod, some energy losses are expected to reduce amplitude. This attenuation is described by Equation 32.

Figure 15 shows the expected amplitude, as a percent of the total, in the rod of a fully transferred resonant wave at the relevant strain gauge locations. If fully coupled to the horn and not restrained, then it is expected that no displacement would be measured at the ¼ and ¾ locations and that the displacement at the ½ wavelength location would be nearly the same as the input amplitude.

For this experiment, data was gathered at the test conditions listed in Table 2. Multiple rod geometries, loads, and amplitudes were selected so that the effect of each variable on the measured displacement in the rod could be analyzed. The chosen loads were selected because they are similar to those used in typical ultrasonic welding applications. The amplitudes selected were small enough to prevent melting so that the tests could be duplicated.

The expected displacement in each strain gauge, ΔL, based solely on the static load applied, can be calculated per Equation 54:

$$\Delta L = \frac{FL}{EA} \quad (54)$$

where F is the applied load, L is the total length of the gauge, E is the elastic modulus, and A is the cross-sectional area of the rod.

For an applied force of 2224 N, a strain gauge length of 0.635 cm, a radius of 1.27 cm (area of 5.07 sq.cm), and an elastic modulus of 2275 MPa, the displacement in the strain gauge is expected to be:

$$\Delta L = \frac{2224 * 0.635}{227500 * 5.07} = .0012\text{ cm} = 12\ \mu\text{m} \quad (55)$$

For a force of 890 N, a strain gauge length of 0.635 cm, a radius of 1.27 cm (area of 5.07 sq.cm), and an elastic modulus of 2275 MPa, the displacement in the strain gauge is expected to be:

$$\Delta L = \frac{890 * 0.635}{227500 * 5.07} = .00049\text{ cm} = 4.9\ \mu\text{m} \quad (56)$$

For a force of 2224 N, a strain gauge length of 0.635 cm, a radius of 0.635 cm (area of 1.27 cm^2), and an elastic modulus of 2275 MPa, the displacement in the strain gauge is expected to be:

$$\Delta L = \frac{2224 * 0.635}{227500 * 1.27} = .0049\text{ cm} = 49\ \mu\text{m} \quad (57)$$

Results

The average displacement measured for each of the experimental conditions and the calculated elastic displacement, shown by the red line, are shown in Fig. 16. Each measurement was taken three times, with the exception of the 39 micron amplitude test on the 0.635-in.-radius rod at 2224 N, which was only tested once.

The calculated elastic displacement for the 2.54-cm-diameter rod under high load matched the measured displacement well. The measurements are a bit further off for the other conditions. This discrepancy is likely due to an estimated elastic modulus used from literature rather than a measurement of the value for these specific rods. However, for all welding trials, the modulus of the material used was tested directly.

For all the strain test conditions, the measured displacements with and without ultrasonic vibration are very close. The displacement measured by the strain gauge is not significantly affected by the addition of ultrasonic vibration. However, changes in the material geometry and the applied load strongly affect it.

These results may suggest that the strain gauges could not measure the oscillations due to the applied ultrasonic vibration. However, the oscillation due to vibration is apparent when the displacement is graphed vs. time for a cycle with and without ultrasonics. This can be seen in the displacement vs. time graphs at the lower force of 890 N — Figs. 17 and 18.

The displacement response is nearly the same with and without the addition of ultrasonic vibration. The biggest difference is that, with ultrasonics, once the maximum load has been reached, the displacement oscillates around the constant displacement measured when there are no ultrasonic vibrations. This is true for both the ¼ wave and ½ wave locations. While there should be no displacement at the node, in the ¼ wave location, the strain gauge covers a much larger area of the rod than a single node.

This data supports the hypothesis that the displacement in the polymer is limited by the geometry and force, even

when more ultrasonic amplitude is applied than the calculated elastic displacement, as was the case for the trial performed on the 2.54-cm-diameter rod at 200 lb, which is seen in Fig. 19. We note that these strain gauges have been placed in the main body of specimens and not at an energy director where large stress concentration exists. The strain gauge results only prove our hypothesis that energy losses at the main body of the specimens to be welded are minimal and that mostly elastic deformations of these areas can be assumed.

The small cross-sectional area of the designed joint, such as an energy director, where a large stress concentration exists, increases the deformation and results in faster heating of such a small volume of material. At the beginning of the weld, the small point of the energy director means that the displacement is larger than the amplitude at the joint, helping melt initiation, which requires the most energy.

Summary

Ultrasonic welding is the most-used polymer welding process. It is widely applicable in the medical, electronics, consumer, and automotive industries. It is important to understand the heating mechanisms at work in this process to design parts for welding properly and to select proper welding parameters.

It was hypothesized that the traditional approach to estimating strain at the weld, based purely on the amplitude of the ultrasonic vibration at the joint, was imperfect. It was proposed that the elastic deformation defined by the part's geometry and the load applied would limit the actual strain produced in the system. This was validated through the experimental trials described, which showed that the strain in the parts during ultrasonic vibration oscillated around the strain that was recorded when no vibration was applied.

In this paper, the physical and material property contributions to polymer heating during ultrasonic excitation have been thoroughly discussed and equations to account for all factors proposed. The updated approach to estimating strain allows for the part geometry and the force being applied during welding to be taken into account in addition to the amplitude of the ultrasonic wave applied. This approach accounts for observable phenomena that previous approaches did not.

The following formulae have been proposed:

Amplitude at distance (x) from the horn contact surface:

$$A(x) = A_0 \cos\left(\frac{-2\pi x}{\lambda}\right) e^{\frac{-\pi x E''}{\lambda E^*}} \quad (58)$$

where A(x) is the function of maximum peak-to-peak amplitude as a function of distance into the material, A_0 is the peak-to-peak amplitude at the sonotrode contact surface, λ is the wavelength in the polymer, E'' is the loss modulus, and E* is the complex modulus.

Deformation of the energy director:

$$\delta x = \frac{F}{E}\frac{h}{bL}\ln\left(\frac{x}{h}\right) \quad (59)$$

where F is the force applied, h is the energy director height, E is the elastic modulus, b is the energy director width, and L is the energy director length.

Acknowledgments

The researchers would like to thank Matt Nitsch for his excellent technician support.

References

1. Levy, A., Le Corre, S., and Villegas, F. 2014. Modeling of the heating phenomena in ultrasonic welding of thermoplastic composites with flat energy directors. *Materials Processing Technology* 214: 1361–1371.

2. Grewell, D., Benatar, A., and Park, J. 2003. *Plastics and Composites Welding Handbook*.

3. Potente, H., Fiegler, G., Haterkamp, H., Fargas, M., von Busse, A., and Bunte, J. 2006. An approach to model the melt displacement and temperature profiles during the laser through-transmission welding of thermoplastics. *Polymer Engineering and Science* 46: 1565–1575.

4. Himenz, P., and Lodge, T. 2007. Crystalline polymers. *Polymer Chemistry*.

5. Tadmor, Gogos. 2006. *Principles of Polymer Processing*.

6. Sancaktar, E. 1999. Polymer adhesion by ultrasonic welding. *Journal of Adhesion Science and Technology* 13(2): 179–201.

7. Suresh, K., Roopa Rani, M., Prakasan, K., and Rudramoorthy, R. 2007. Modeling of temperature distribution in ultrasonic welding of thermoplastics for various joint designs. *Journal of Materials Processing Technology* 186: 138–146.

8. Krautkrammer, J., and Krautkrammer, H. 1993. Chapter 6: Attenuation of ultrasonic waves in solids. *Ultrasonic Testing of Materials*: 108–116.

9. Benatar, A., and Cheng, Z. 1989. Ultrasonic welding of thermoplastics in the far-field. *Journal Polymer Engineering Science* 29(23): 1699–1704.

10. Gallego-Juarez, J., and Graff, K. 2015. *Power Ultrasonics: Applications of High Intensity Ultrasound*.

11. Marcus, M., Anantharaman, S., and Aldaz, B. 2013. Advantages of a servo-driven ultrasonic welder. *ANTEC*.

12. Grewell, D., and Benatar, A. 2008. Semi-empirical, squeeze flow, and intermolecular diffusion model. II. Model verification using laser microwelding. *Polymer Engineering and Science* 48(5): 543–1549.

13. Hopmann, C., Dahlmann, R., Weihermuller, M., Wipperfurth, J., and Sommer, J. 2022. Determination of the frequency and temperature dependent stiffness and damping properties of thermoplastics for the prediction of the vibration and heating behaviour during ultrasonic welding. *Welding in the World* 67(1).

14. Chuah, C., and Chang, L. 2000. Effects of the shape of the energy director on far-field ultrasonic welding of thermoplastics. *Polymer Engineering and Science* 40(7): 157–167.

15. Ueda, K., and Umeda, A. 1998. Dynamic response of strain gauges up to 300 kHz. *Experimental Mechanics* 38(2): 93–98.

MIRANDA MARCUS (*mmarcus@ewi.org*) is with the Edison Welding Institute, Columbus, Ohio, and **EROL SANCAKTAR** is with the University of Akron, Akron, Ohio.